Research Article

Optimization of Reinforced Aluminium Scraps from the Automobile Bumpers with Nickel and Magnesium Oxide in Stir Casting

V. Vijayan,[1] A. Parthiban,[2] T. Sathish ⓘ**,[3] L. Ponraj Sankar,[4] S. Dinesh Kumar,[5] S. Saravanakumar,[6] and Dawit Tafesse** ⓘ**[7]**

[1]*Department of Mechanical Engineering, K. Ramakrishnan College of Technology (Autonomous), Samayapuram, Trichy 621 112, Tamil Nadu, India*

[2]*Department of Mechanical Engineering, Vels Institute of Science, Technology & Advanced Studies, Pallavaram, Chennai 600 117, Tamil Nadu, India*

[3]*Department of Mechanical Engineering, Saveetha School of Engineering, SIMATS, Chennai 602 105, Tamil Nadu, India*

[4]*Department of Civil Engineering, CMR Institute of Technology, Hyderabad, India*

[5]*Department of Mechanical Engineering, St. Peter's Institute of Higher Education and Research, Avadi, Chennai 600 054, Tamil Nadu, India*

[6]*Department of Mechanical Engineering, M.Kumarasamy College of Engineering, Karur, Tamil Nadu, India*

[7]*Department of Mechanical Engineering, Faculty of Manufacturing, Institute of Technology, Hawassa University, Hawassa, Ethiopia*

Correspondence should be addressed to Dawit Tafesse; dawitt@hu.edu.et

Here, the investigation is spotlighted on the aluminium alloy from the waste materials of the automobile bumpers which is a reinforced metal matrix composite created with 5 percentage of nickel and 5 percentage of magnesium oxide through the stir casting method. The stir casting process inputs parameters such as pressure of squeezing, time of squeezing, and speed of stirrer which were optimized based on the two mechanical properties' outcome such as the tensile strength (TS) and Rockwell hardness. There are nine different experiments which were conducted based on the L9 array. The Taguchi method is used to identify the optimum input values for the greatest result of the processing condition by Minitab software. The responses-based parameters were ordered based on the rank identified through the investigational effects. Finally, the optimized input consideration values and the linear equations are recommended for both the considered outputs as conclusions.

1. Introduction

Around the world, scraps of the automobiles are increased day by day, so the effective utilization of the wastes of automobiles, such as accidental bodies, damaged bodies, and replaced bodies, can be reusable after recycling. Here, especially the automobile bumpers which are made up of aluminium were chosen for this investigation. Christy et al. [1] completely explained about optimization techniques used for the input parameters of the squeeze and stir casting

with the help of the Taguchi technique. They also explained with the various microstructure diagrams and comparison plots. They used the four input parameters for the four output responses. The basic things of the optimization techniques for the various machining processes of composites such as various proportions of aluminium with zirconium carbide composite [2], several combinations of aluminium with silicon carbide [3], and numerous combinations of aluminium with nanomaterials [4] in the same way machining such as parameters of the laser welding

process [5], electrochemical machining process [6], A-GTAW welding [7], diffusion bonding process [8], turning process on the Lathe machine [9]. Krishnan et al. [10] discussed fully about the metal matrix composites which are produced from the aluminium scrap and materials from the wastes. They give the justification and implementation idea about the various techniques used for the production from those wastes and the scraps. They also defended based on the microstructures and also with characteristics of the composite material with the preliminary materials. Gesing et al. [11] clearly discussed regarding the light metals recycling through the used vehicles and life-ended vehicles' parts and scraps. These recommendations provide confidence to create this type of the research work. Similarly, Gupta et al. [12] reviewed through various research articles and explained about the process of solidification of metal matrix composites. In this investigation mainly focused with the used or damaged or scraped aluminium automobile bumpers recycling with the reinforcement then the optimization undergo with the basic mechanical properties like tensile strength and hardness based input parameters. Alaneme et al. [13] successfully explained regarding the creation in addition age-hardening accomplishment of aluminium composite through silicon carbide for the formation of composite through stir casting method.

Mohan et al. [14] explained the mechanical properties-based optimization of the parameters on the aluminium composites. Pawar et al. [15] professionally investigated about spur gear-based composite of aluminium reinforcement with silicon carbide. They fully expressed the different application with perfect experimental discussion with different figures. Evangelia Georgantzia et al. [16] exclusively clarified concerning AA6XXX series numerous applications with regard to more than a few sizes of physical components in dissimilar forms, process of welding, and equipment through bolted places of equipment. Weiwei et al. [17] investigated about the wheel hub of aluminium alloy failure-based analysis with various simulations. They mentioned the importance of the bumpers as follows: it is accomplished of enduring influences at 2 mph through complete breadth and 1 mph on bends. The bumper must be adept of tolerating influences to prevent 5 mph crashes of the automobiles. Vousden [18] mentioned about the Ferrari about its bumper shape made up of aluminium which is stress-free fiber of carbon composites with neglectable weight. Zhang et al. [19] investigated about the aluminium alloy of 7003 based on the stress corrosion with respect to the automobile vehicles. They also focused on the bumpers made up of aluminium with merits and demerits. These aluminium bumpers were less in weight and more strong when compared to steel. Weiwei et al. [17] discussed about automobile parts-based examination such as breakage of the wheel made up of the aluminium alloy with the various simulations and recommendations of the recycling of the used and damaged automobile parts. Vijay Kumar et al. [20] entirely examined various magnesium-based research articles and they provided the maximum information about the composites of biodegradable magnesium . They also gave the importance for the attention with properties and their availability, usages

on the environment. The biodegradable magnesium composites had the advanced strength to wear ratio in addition to furthermore articulated microstructure of the composite by means of various SEM pictures.

Abhijit et al. [21] completely reviewed by means of more than sixty research articles regarding the composite of the magnesium with various combinations of alloys. They concluded that the magnesium is used to strengthen the engineering materials with numerous fabrication methods and also they gave details about the reinforcement influence on the magnesium with additional materials such as silicon carbide, aluminium oxide, boron carbide, titanium carbide, fibers, and carbon nanotubes. This investigation predominantly focused to find the appropriate parameters used to produce the recycling of the scraps or wastes from the automobile bumpers by the way of composite formation with nickel and magnesium oxide in stir casting process. The suitable parameters were considered based on the experimental consequence of furthermost desirable mechanical properties such as tensile strength and hardness of the composite produced by the way of stir casting process.

1.1. Experimental Setup. The waste aluminium bumpers were collected from various mechanic shops and different automobile service centers. Then, some pieces of the entire waste bumper were taken for this investigation and were cleaned and converted into small pieces which are also converted into powder form by pulverizing. It contains 1.1 to 1.7 percentage of silicon, 0.7 to 1.3 percentage of magnesium, 0.8 to 1.18 percentage of copper, 0.7 to 1.2 percentage of manganese, and 0.5 percentage of chromium in the total composition. Then, the cleaned aluminium majorly used then the five percentage of nickel and five percentage of magnesium oxide reinforce in the total volume of the composite metal.

The stir casting setup used for this experimental trail is bottom pouring method. It contains the control panel, electrical furnace, runway preheater, die, reinforcement preheating chamber, and hydraulic sequence pressure ram. Initially, the pieces of the automobile bumpers and the nickel and magnesium were placed in the stir casting place, as shown in Figure 1. As shown in Table 1, there are nine experimental trails which created hydraulic squeeze pressures considered as 80 MPa, 100 MPa, and 120 MPa. The sintering speed varies from 400 rpm, 500 rpm, and 600 rpm. The time of the squeeze varied as 20 sec, 40 sec, and 60 sec. The holding pressure was maintained as 300ºC throughout all experiments.

As shown in Table 1, the specimens were formed as per the size of 30 mm × 30 mm × 120 mm as width, length, and height by bottom pouring on the mold. There are nine specimens prepared with pressure, time, and speed variations for the specimens. Then, the specimens were used to take the tensile strength as per the traditional method in the universal testing machine as per the standards. Then, the tensile strength was noted for each specimen. Similarly, the Rockwell hardness machine with the diamond intender cone is used to identify the hardness of each specimen and the corresponding values were noted.

FIGURE 1: The friction stir machine setup used.

TABLE 1: Experimental trails of design.

Experimental trail No.	Pressure (P) (MPa)	Time (t) (s)	Speed (N) (rpm)
ET 1	80	20	400
ET 2	80	40	500
ET 3	80	60	600
ET 4	100	20	500
ET 5	100	40	600
ET 6	100	60	400
ET 7	120	20	600
ET 8	120	40	400
ET 9	120	60	500

2. Results and Discussion

The measured values of the tensile strength and the hardness values are clearly mentioned in Table 2 for all the experimental trails. Here, the Taguchi technique was implemented for both tensile strength and hardness separately and jointly. For all these three conditions, larger is better condition which is used for the processing in the Minitab-18 software.

Individual plots and combination plots were utilized to identify the real impact on the experimental results.

Figure 2 shows the tensile strength foremost result diagram for ratio of SN and Figure 3 shows the tensile strength foremost result diagram for ratio of means clearly. From these two diagrams, the maximum output is obtained in the range for pressure of squeezing is 120 MPa, time of squeezing is 60 sec, and speed of stirrer is 400 rpm. Table 3

TABLE 2: Results of the experiments.

Experimental trail No.	Pressure (P) (MPa)	Time (t) (s)	Speed (N) (rpm)	Tensile strength (MPa)	Hardness (HRB)
ET 1	80	20	400	128.48	49.82
ET 2	80	40	500	133.98	51.26
ET 3	80	60	600	139.48	52.7
ET 4	100	20	500	121.2	46.1
ET 5	100	40	600	126.7	47.54
ET 6	100	60	400	169.7	62.66
ET 7	120	20	600	113.92	42.38
ET 8	120	40	400	156.92	57.5
ET 9	120	60	500	162.42	58.94
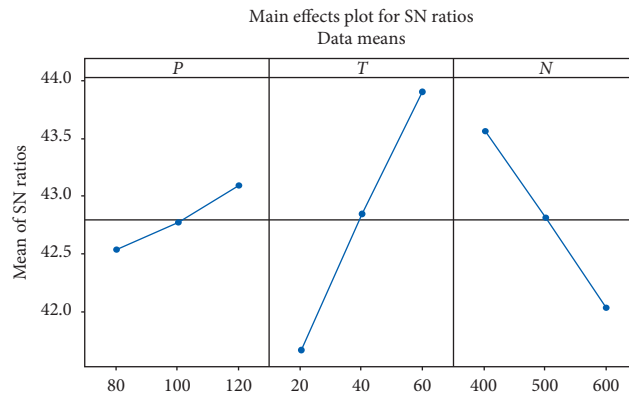
FIGURE 2: Tensile strength: foremost result diagram for ratio of SN (in X axis, P is the pressure in MPa, T is the time in s, and N is the speed in rpm).
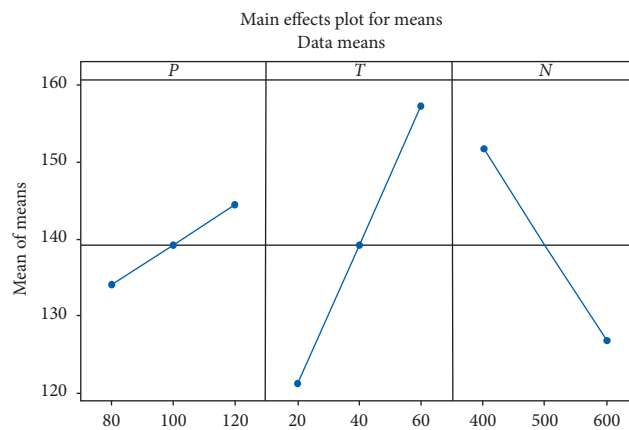

FIGURE 3: Tensile strength: foremost result diagram for ratio of means (in X axis, P is the pressure in MPa, T is the time in s, and N is the speed in rpm).

details about the responses for SN ratio and means for the tensile strength; from that response table, the most impact crated factor is time of squeezing; secondly, it is speed of stirrer, and the last parameter is pressure of squeezing. Table 4 shows variance analysis provided that the minimum "P" values which express the reliability of the experiments and parameters are considered.

Figure 4 shows the three different plots of contour diagram in a single plot. It contains the contour diagrams of the time verses pressure, speed verses pressure, and then speed verses time. The variations were represented as the color variations which are clearly represented in the right side of the diagram; each range has a different color for the representations. Figure 5 represents the histogram diagram for the tensile strength with respect to the frequencies which have the mean as 139.2 MPa and standard deviation of 19.51.

The probability plot is shown in Figure 6 with respect to the tensile strength which is represented in X axis and percent is mentioned in the Y axis. In this diagram, entire values were near to the mean line of the plot nearly four to

TABLE 3: Tensile strength response table.

Level	Response for SN ratio			Response for means		
	P (MPa)	t (s)	N (rpm)	P (MPa)	t (s)	N (rpm)
1	42.54	41.66	43.56	134.0	121.2	151.7
2	42.77	42.84	42.81	139.2	139.2	139.2
3	43.09	43.90	42.03	144.4	157.2	126.7
Delta	0.55	2.24	1.54	10.4	36.0	25.0
Rank	3	1	2	3	1	2

TABLE 4: Tensile strength variance analysis for SN ratios.

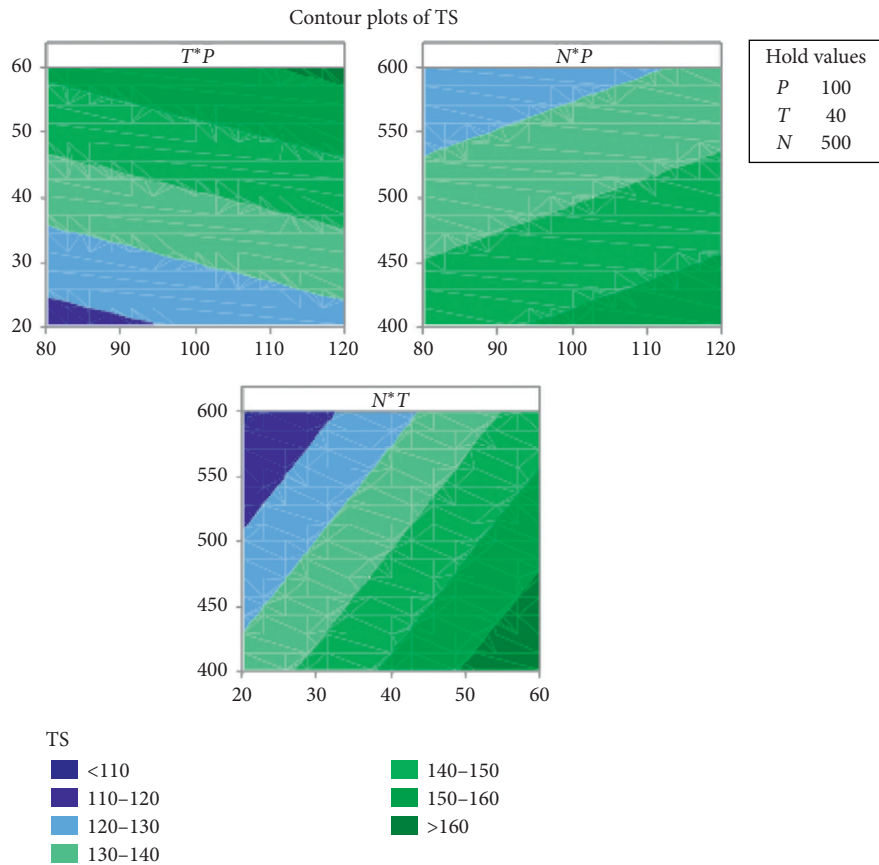| Source	DF	Seq SS	Adj SS	Adj MS	F	P value
P (MPa)	2	0.4570	0.45696	0.22848	54.29	0.018
t (s)	2	7.5283	7.52829	3.76415	894.43	0.001
N (rpm)	2	3.5365	3.53650	1.76825	420.17	0.002
Residual error	2	0.0084	0.00842	0.00421		
Total	8	11.5302				

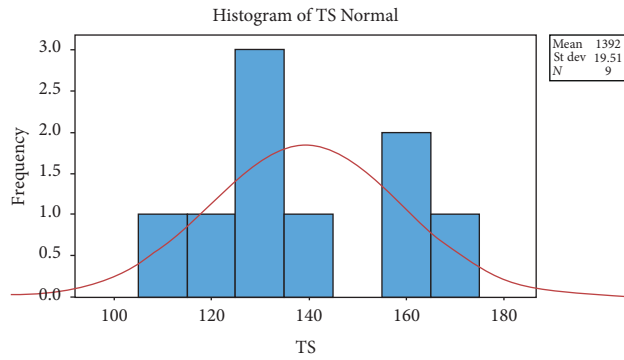FIGURE 4: Contour diagrams for tensile strength (P, pressure in MPa; T, time in s; N, speed in rpm).

Histogram of TS Normal

FIGURE 5: Tensile strength responses as histogram (X axis: TS in MPa and Y axis: frequency in Hz).

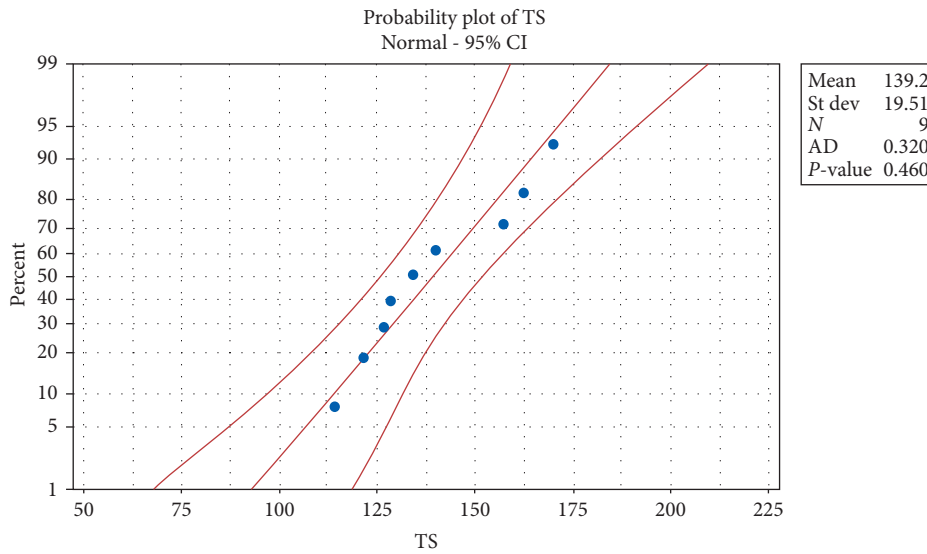Probability plot of TS
Normal - 95% CI

FIGURE 6: Tensile strength responses as probability plot (X axis: TS in MPa and Y axis: %).

five points' lies on the mean line. By using the regression, the following equation is formed for the tensile strength with respect to the contribution considerations:

$$\text{regression equation for tensile strength} = \text{TS} = 139.6 + 0.2610P + 0.9000T - 0.1250N. \tag{1}$$

The experimental results of the hardness-based foremost result diagram for ratio of SN and means of date are plotted in Figures 7 and 8, respectively; in the same order, these experiments analysed based on the condition of larger is better. The optimum input parameters for the upper most results of the harness were 120 MPa of the pressure of squeezing, 60 sec time of squeezing, and 400 rpm speed of stirrer. These values were also confirmed by both the SN ratio-based diagram and means-based diagram.

The corresponding response table based on the SN ratio and means is shown as Table 5 with the condition of larger is better. For both the conditions, time reached the rank one, speed of stir reached the second rank, and the holding pressure reached the last rank among these three parameters based on the experimental results of the hardness. Similarly, Table 6 lists the variation of the analysis for the hardness results based on the SN ratio. The P value is less than 0.2 for all the parameters, especially time and speed have very low value of the P value in Table 6.

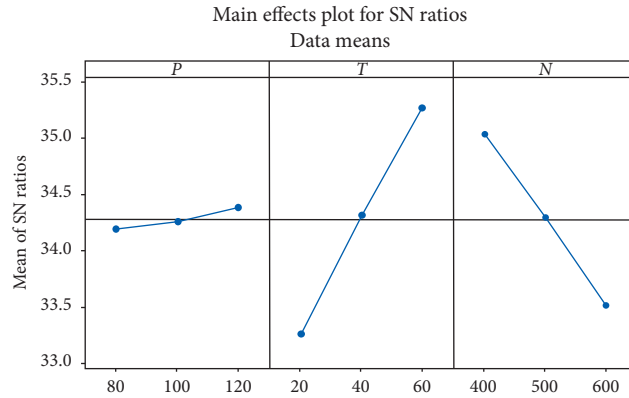$$\text{Regression equation for hardness (HRB)} = 58.70 + 0.04200P + 0.3000T - 0.04560N. \tag{2}$$

FIGURE 7: Hardness: foremost result diagram for ratio of SN (in X axis, P is the pressure in MPa, T is the time in s, and N is the speed in rpm).

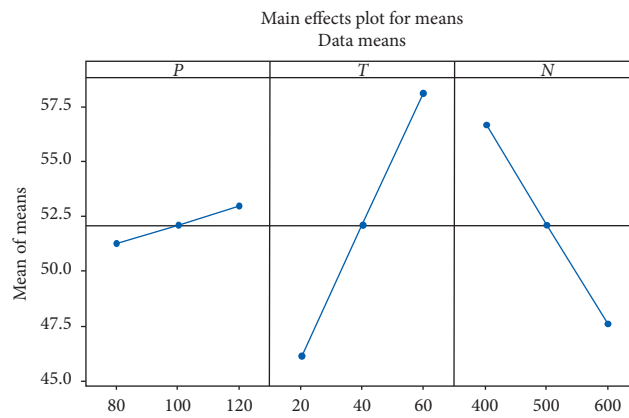FIGURE 8: Hardness: foremost result diagram for means (in X axis, P is the pressure in MPa, T is the time in s, and N is the speed in rpm).

TABLE 5: Hardness response table with ranks.

Level	Response for SN ratio			Response for means		
	P (MPa)	t (s)	N (rpm)	P (MPa)	t (s)	N (rpm)
1	34.19	33.26	35.03	51.26	46.10	56.66
2	34.25	34.31	34.29	52.10	52.10	52.10
3	34.38	35.26	33.51	52.94	58.10	47.54
Delta	0.19	2.01	1.52	1.68	12.00	9.12
Rank	3	1	2	3	1	2

TABLE 6: Analysis of variance of hardness for ratios of SN.

Source	DF	Seq SS	Adj SS	Adj MS	F	P value
P (MPa)	2	0.05575	0.05575	0.02787	5.09	0.164
t (s)	2	6.04324	6.04324	3.02162	551.85	0.002
N (rpm)	2	3.46786	3.46786	1.73393	316.67	0.003
Residual error	2	0.01095	0.01095	0.00548		
Total	8	9.57780				

Figure 9 provides the details of the experimental results of the hardness as the contour plot depends on the parameter variations in a single diagram with the color variations for the identification of the range variation on the results. Similarly, the histogram view of the experimental outcomes of the hardness values is clearly plotted in

Figure 10 with linear relation curve. There is no gab in between the columns available on the histogram diagram. The probability chart for the harness results is plotted in Figure 11. All the experimental values nearly closer the median line on the chat. Nearly six to seven points were nearly close to the median line.

In Table 7, the confirmation test is created with the combination of the both tensile and harness strength based foremost result diagram for ratio of SN is shown in Figure 12, and the foremost result diagram for data means is shown in Figure 13; similarly, response table with ranks based on SN ratios is shown as Table 6. As shown in Figures 12 and 13, the maximum output of both the mechanical properties reached higher values at the pressure of squeezing 120 MPa, time of squeezing 60 sec, and speed of stirrer
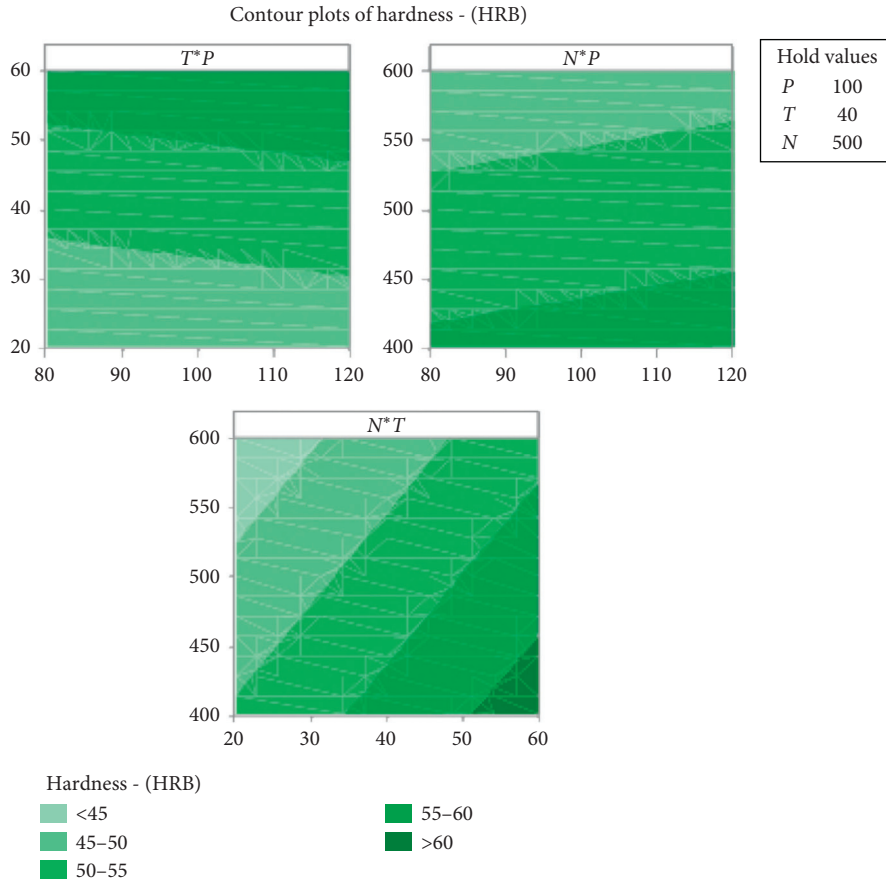
Contour plots of hardness - (HRB)

FIGURE 9: Hardness-contour plot depends on the parameters variations (P, pressure in MPa; T, time in s; N, speed in rpm).
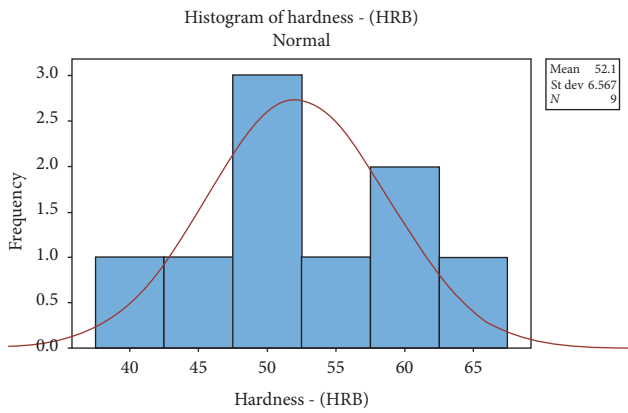

FIGURE 10: Hardness: histogram diagram (X axis: TS in MPa and Y axis: frequency in Hz).

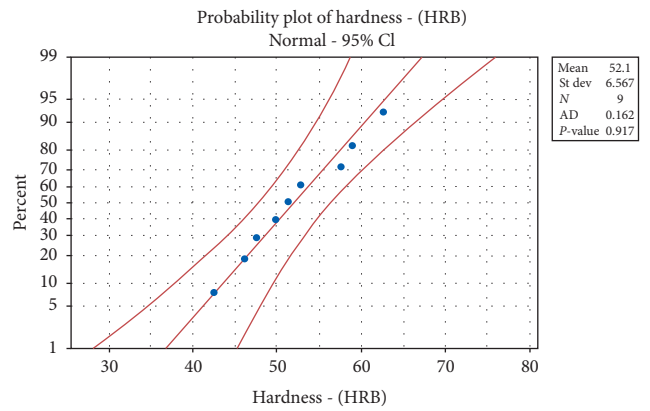

FIGURE 11: Hardness: probability plot (X axis: TS in MPa and Y axis: %).

TABLE 7: Tensile strength and harness-based response table with ranks based on SN ratios.

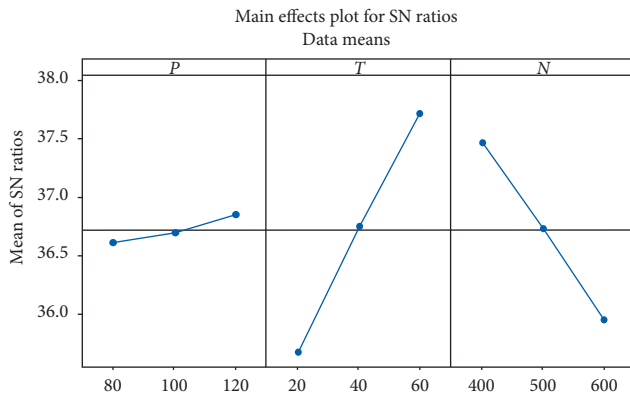| Level	P (MPa)	t (s)	N (rpm)
1	36.61	35.68	37.47
2	36.69	36.75	36.73
3	36.84	37.71	35.95
Delta	0.23	2.04	1.52
Rank	3	1	2

FIGURE 12: Both tensile strength and harness-based foremost result diagram for ratio of SN (In X axis, P is the pressure in MPa, T is the time in s, and N is the speed in rpm).
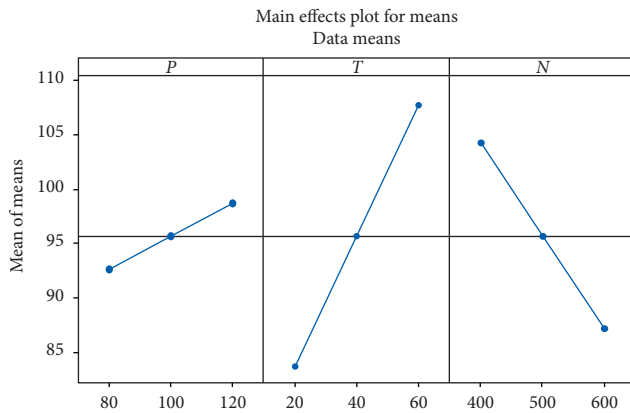

FIGURE 13: Both tensile strength and harness-based foremost result diagram for data means (In X axis, P is the pressure in MPa, T is the time in s, and N is the speed in rpm).

400 rpm. The corresponding ranking is obtained in the order of time, speed, and pressure as first, second, and third.

3. Conclusions

This optimization study of reinforced aluminium scraps from the automobile bumpers with nickel and magnesium oxide in stir casting gave the following results as conclusions:

(i) The recycling of the aluminium automobile bumpers into the reinforced composite is possible.

(ii) For the experimental results of the tensile strength, hardness and both combination conditions

response table gave the first rank for time of squeezing, the second rank for speed of stirrer, and the third rank for holding pressure.

(iii) The regression equations (1) and (2) were created for tensile strength and hardness with respect to the same conditions, respectively.

(iv) Both the enhanced mechanical properties were obtained at the input parameters such as pressure of squeezing 120 MPa, time of squeezing 60 sec, and speed of stirrer 400 rpm.

(v) The optimized contribution concern values and the linear equations are recommended for tensile strength and hardness.

(vi) Further scope of this work was extended to conduct the impact test for the same material with increase of the reinforcement for preventing the impact of accident to the vehicle.

Data Availability

The data used to support the findings of this study are included within the article. Further data or information is available from the corresponding author upon request.

Disclosure

This study was performed as part of employment in Hawassa University, Ethiopia.

Conflicts of Interest

The authors declare that there are no conflicts of interest regarding the publication of this paper.

Acknowledgments

References

[1] J. V. Christy, R. Arunachalam, A.-H. I. Mourad, P. K. Krishnan, S. Piya, and M. Al-Maharbi, "Processing, properties, and microstructure of recycled aluminum alloy composites produced through an optimized stir and squeeze casting processes," *Journal of Manufacturing Processes*, vol. 59, pp. 287–301, 2020.

[2] T. Sathish and N. Sabarirajan, "Synthesis and optimization of AA 7175 - Zirconium Carbide (ZrC) composites machining parameters," *Journal of New Materials for Electrochemical Systems*, vol. 24, no. 1, pp. 34–37, 2021.

[3] T. Sathish, N. Sabarirajan, and S. Karthick, *Materials Today Proceedings*, Elsevier Publisher, Netherlands, Accepted, 2019.

[4] T. Sathish, K. Muthukumar, R. Saravanan, and V. Dhinakaran, "Study on temperature difference of aluminium nitride nanofluid used in solar flat plate collector over normal water," *AIP Conference Proceedings*, vol. 2283, no. 1, AIP Publishing LLC, Article ID 020126, 2020.

[5] R. Karthick, K. Adithya, C. Hariharaprasath, and V. Abhishek, "Evaluation of mechanical behavior of banana fibre reinforced hybrid epoxy composites," *Materials Today: Proceedings*, vol. 5, no. 5, pp. 12814–12820, 2018.

[6] T. Sathish, "Experimental investigation of machined hole and optimization of machining parameters using electrochemical machining," *Journal of Materials Research and Technology*, vol. 8, no. 5, pp. 4354–4363, 2019.

[7] T. Sathish, S. Dinesh Kumar, K. Muthukumar, and S. Karthick, "Natural inspiration technique for the parameter optimization of A-GTAW welding of naval steel," *Materials Today: Proceedings*, vol. 21, pp. 843–846, 2020.

[8] T. Sathish, S. Dinesh Kumar, K. Muthukumar, and S. Karthick, "Temperature distribution analysis on diffusion bonded joints of Ti-6Al-4V with AISI 4140 medium carbon steel," *Materials Today: Proceedings*, vol. 21, pp. 847–856, 2020.

[9] S. P. Palaniappan, K. Muthukumar, R. V. Sabariraj, S. Dinesh Kumar, and T. Sathish, "CNC turning process parameters optimization on aluminium 6082 alloy by using Taguchi and ANOVA," *Materials Today: Proceedings*, vol. 21, pp. 1013–1021, 2020.

[10] P. K. Krishnan, J. V. Christy, R. Arunachalam et al., "Production of aluminum alloy-based metal matrix composites using scrap aluminum alloy and waste materials: influence on microstructure and mechanical properties," *Journal of Alloys and Compounds*, vol. 784, pp. 1047–1061, 2019.

[11] A. Gesing and R. Wolanski, "Recycling light metals from end-of-life vehicle," *Journal of Occupational Medicine*, vol. 53, no. 11, pp. 21–23, 2001.

[12] N. Gupta and K. G. Satyanarayana, "Symposium review: solidification processing of MMCs," *Journal of Materials Science*, vol. 58, no. 6, pp. 91–93, 2006.

[13] K. K. AlanemeaΨ and A. O. Alukob, "Production and age-hardening behaviour of borax premixed SiC reinforced Al-Mg-Si alloy composites developed by double stir-casting technique," *The West Indian Journal of Engineering*, vol. 34, no. 1, p. 2, 2012.

[14] T. R. Mohan, C. M. Sharanaprabhu, and S. K. Kudari, "Study on the effects of SiC particles on tensile properties for Al/SiC composites," *International Journal of Services Technology and Management*, vol. 4, pp. 2394–1537, 2015.

[15] P. B. Pawar and A. A. Utpat, "Development of aluminium based silicon carbide particulate metal matrix composite for spur gear," *Procedia Materials Science*, vol. 6, pp. 1150–1156, 2014.

[16] E. Georgantzia, M. Gkantou, and G. S. Kamaris, "Aluminium alloys as structural material: a review of research," *Engineering Structures*, vol. 227, Article ID 111372, 2021.

[17] W. Song, J. L. Woods, R. T. Davis et al., "Failure analysis and simulation evaluation of an Al 6061 alloy wheel hub," *Journal of Failure Analysis and Prevention*, vol. 15, no. 4, pp. 521–533, 2015.

[18] M. Vousden, "Car materials- what they are andd what they'regood for," carwow. [Online]. Available: http://www.carwow.co.uk/blog/Car-Materials-Explained, 2015.

[19] S. Zhang, X. Wang, H. Chen, and X. Liao, "Stress corrosion cracking of cabinet of 7003 aluminum alloy," *Cailiao Gongcheng/Journal of Materials Engineering*, vol. 43, no. 7, pp. 105–112, 2015.

[20] B. Vijay Kumar and C. T. R. Mallarapu Gopi Krishna, "Magnesium matrix composites for biomedical applications: a review," *Journal of Magnesium and Alloys*, vol. 7, pp. 72–79, 2019.

[21] V. K. Bommala, M. Krishna, and C. Rao, "Magnesium metal matrix composites - a review," *Reviews on Advanced Materials Science*, vol. 42, no. 1, pp. 58–67, 2015.